Chemical Science & Engineering Research

Ariviyal Publishing

Research Article

DOI: 10.36686/Ariviyal.CSER.2021.03.08.035

Chem. Sci. Eng. Res., 2021, 3(8), 1-6.

Structural, Optical and Morphological Properties of Polymer Inorganic Composite Thin Films: Applications

Karabasappa H Byadgi

Department of Chemistry, KLE Society's Gudleppa Hallikeri College, Haveri – 581 110, Karnataka, India.

***Corresponding author E-mail address**: khbyadagi12@gmail.com

ISSN: 2582-3353

Crossref

Publication details
Received: 24th August 2021
Revised: 18th October 2021
Accepted: 18th October 2021
Published: 02nd November 2021

Abstract: This Paper presents the results of the Polymer-Inorganic (PVA-ZnO) composite thin films were prepared by solution casting method, the samples were characterized by different characterization techniques by XRD, FTIR, UV–visible spectroscopy, Mechanical and Morphological. Also, we had studied the optical properties of PVA/ZnO composites based on ZnO as inorganic filler material and PVA as the main matrix. The main aim is to prepare Poly Polyvinyl alcohol/Zinc Oxide nanoparticles biopolymer nanocomposite (PVA/ZnO) and to study its behaviour for different concentrations of ZnO. Here, ZnO of average size 100 nm was used. The physical, mechanical, surface, and antibacterial properties of PVA/ZnO (100 nm) Bio thin films have been discussed in detail here and how the physical modifications of PVA, due to ZnO incorporation, will bring changes in the other properties.

Keywords: PVA-ZnO; XRD; FTIR; UV-Vis; AFM

1. Introduction

A polymer is a macromolecule, consisting of a chain of smaller organic molecules, called as monomers. Due to their wide range of versatile properties, they play an essential role in the daily life of mankind. Polymers can be broadly classified into two types, natural and synthetic polymers. Poor mechanical strength, rapid degradation, and less control over the physical and chemical properties of these polymers have led to the production of artificial polymers, which are usually synthesized from petro-chemicals. These manmade polymers, namely, Low Density Polyethylene (LDPE), High-Density Polyethylene (HDPE), Polypropylene (PP), Polyvinyl Chloride (PVC), Polystyrene (PS), Nylon, Teflon, Thermoplastic Polyurethane (TPU), etc., which are designed and synthetically produced for some desired applications, are called as synthetic polymers. Based on their basic properties, these synthetic polymers are further classified as thermoplastics, thermosets, elastomers, and synthetic fibres.

Synthetic polymers, used as primary packaging in the food industry, are made entirely from chemicals derived from crude oil and are widely used due to its large availability at a relatively low cost.[1] To overcome the environmental problems created by these synthetic non-degradable plastics, researchers have shown an interest in the production of polymers from renewable sources like animals products and agro-wastes.[2-3] These polymers are in fact, synthetically modified natural polymers, and have properties tailored in accordance to the requirements. Since these polymers are derived from living organisms, they are called as biopolymers, and their biocompatibility and biodegradability properties makes them ideal for packaging and bioapplications. Zinc oxide (ZnO) is a transition, inorganic semiconductor material of the II-VI semiconductor group, and is known for its versatile activity in various fields. The bulk and nanoparticles of ZnO materials already has number applications like, additives in rubber, glass, ceramic, plastics, foods, fire extinguishers, paints, ointments, etc. Researchers have found that bulk ZnO has been used in ointment, pigments, and paints by various ancient civilizations. Recently, ZnO nanoparticles are being used on a large scale in the rubber industry, to resist corrosion, and as filler in photocopying papers. ZnO has high absorption of UV light, and hence, it is used commercially as sunscreen in the cosmetics industries in lotions, powders, baby creams, shampoos, etc.; in the rubber industry as UV protectors; in sunglasses and welding glasses to protect eyes from UV ray damage; and in plastics as additive to reduce UV degradations.[4] It is also used as a food additive and has been approved as a generally recorded as safe (GRAS) substance by the Food and Drug Administration (FDA) as being a necessary nutrient source.[5] Due to its wide band gap of 3.37 eV and large extinction binding energy of 60 meV, ZnO has potential application in UV LEDs, laser diodes, solar cells, display screens, photocell

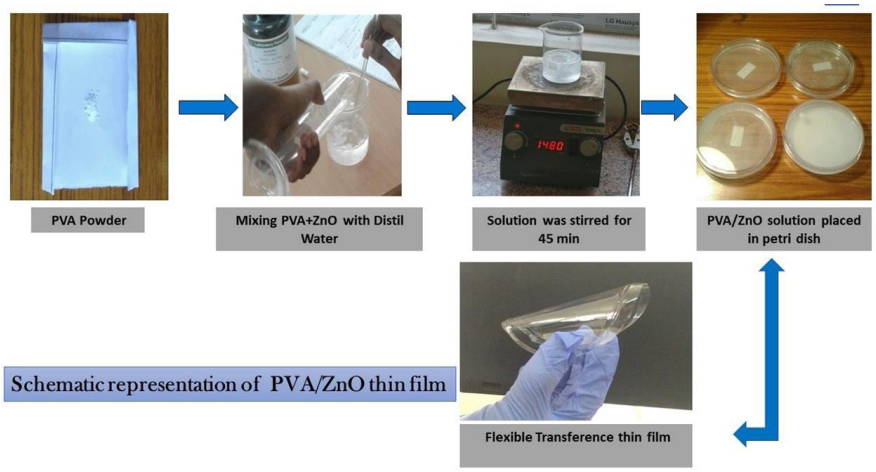

Fig. 1. Schematic representation of PVA/ZnO thin film

electrodes, etc.[6] It can be used as a biomimic membrane and by transfer of fast electrons between electrode and enzyme's active site, it can immobilize or modify proteins.[7-8] ZnO nanoparticles are an environment friendly multifunctional inorganic material and have little toxicity as desirable for bio-applications.[9] It has high surface to volume ratio, chemically alterable physical properties, improved surface reactivity, is thermally stable, and has unique mechanical and electrical properties, which can be varied with size and shape, as well as its synthesis route.[10] The advantages of ZnO over other metal oxide nanoparticles are its low price, photo catalytic activity, good gas sensing properties, antibacterial activity, ease to produce optical materials like photonic crystals, catalytic materials, etc.[11] Researchers have shown that ZnO nanoparticles are biodegradable and biocompatible.[12] The importance of using these inorganic oxide nanoparticles as antimicrobial agents is its effectiveness on the resistant strains of microbial pathogens and less toxicity[13] Since ZnO nanoparticles have antimicrobial properties, it can be used as an additive or dispersive to food packaging material to obtain active food packaging materials.[14]

2. PVA/ZnO thin films Preparation

The Polyvinyl Alcohol/Zinc oxide biopolymer nanocomposites (PVA/ZnO Thin films) were prepared by using the solution casting technique. The commercial grade PVA was obtained from Loba Chemicals, India (E15LV Premium, CAS: 90004-65-3). It is in the form of an odourless white powder. The ZnO powder is used in this work were obtained from Sigma-Aldrich (CAS: 1314-13-2). To prepare the 5 wt% PVA polymer films, 5 g of PVA powder was added to 100 ml of distilled water and stirred for 45 minute at room temperature to obtain a clear viscous solution. Known amounts of ZnO nanopowder (0.01 mg, 0.02 mg, 0.03 mg and 0.04 mg) was added to the 20 ml of viscous PVA solution to prepare different percentages (0.2 wt%, 0.4wt% and 0.6 wt%) of PVA/ZnO Bio-thin films. The mixture solution was stirred for 15 min for uniform dispersion of ZnO, then caste onto glass petri dishes and dried at room temperature to obtain free standing films. A neat PVA without the addition of ZnO was also casted to obtain a free standing film for comparison. The same procedure was followed to prepare different concentrations of PVA/ZnO biopolymer thin films (Fig. 1).

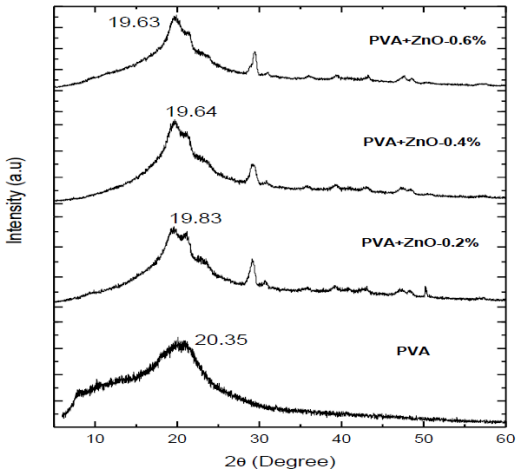

Fig. 2. XRD Scans of PVA/ZnO for different concentrations of ZnO.

3. X-Ray Diffraction Study

X-ray diffractograms for pure and ZnO incorporated PVA films are given in Fig. 2. The pure PVA/ZnO shows a single characteristic peak at 2θ= 20.11º. When the ZnO were added, a peak corresponding to the PVA shifts towards the higher theta value and the diffraction peak becomes broader. This implies that the dispersed and induces changes in the structural properties of the PVA. Since the concentration of ZnO is very less (0.01-0.04 wt%), peaks corresponding to it are not observed, but for higher ZnO concentrations (0.04 wt %), we can observe all peaks at 31.70° and 37.20°. The changes in the structural properties of the PVA after ZnO incorporation were quantified in terms of crystallite size (LXRD), lattice strain (εav), and crystallinity (Xc) of the samples.

The XRD patterns of the polyvinyl alcohol and PVA/ZnO composites films at various weight percentages are shown in Fig. 2. It is suggests that the PVA is amorphous in nature. A peak maximum is observed to be around 20.350 for polyvinyl alcohol, which may be assigned to the scattering between polyvinyl alcohol chains at interplanar spacing. The homogeneously distributed ZnO increases the high surface area of PVA/ZnO composites, leading to increase in the crystallinity of the polymer composites.[15-16] Therefore, the degree of crystallinity of polyvinyl alcohol increases and the diffraction peaks merged into the zinc oxide peaks, which cannot be

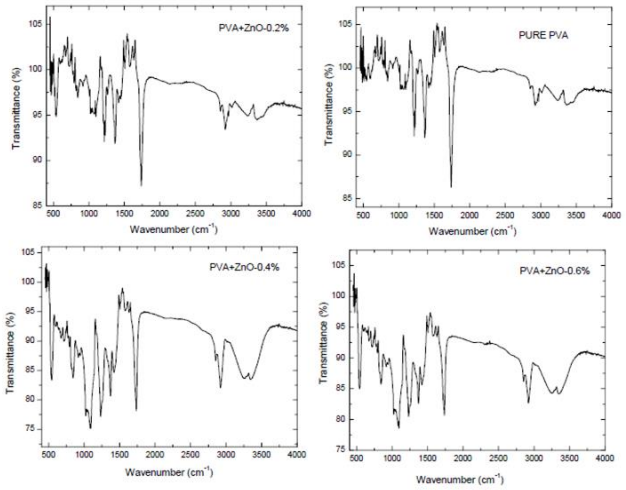

Fig. 3. FT-IR Transmittance curve of PVA/ZnO composite for various wt%.

distinguished. By comparing the XRD patterns of PVA/ZnO composite with that of ZnO, the observed that the plane oriented to (100), (002), (101), (102), (110), (103), (112) and (201) due to corresponding to 2θ = 29.250, 30.630, 36.04 0, 40.350, 43.020, 47.200 and 50.18 0 which shows the presence of zinc oxide in polyvinyl alcohol. The XRD patterns of pure polyvinyl alcohol, ZnO and its composite indicates that ZnO has retained its structure even though it is being capped with PVA after formation of composites. This is due to the weakening of the van der Waal's forces between the polymer molecules, 1) Increase in lattice strain with increase in ZnO concentration, and 2) Decrease in crystallinity of PVA. These changes result in more broadening of the X-ray Bragg's reflections and hence, decrease in the microstructural parameters. On a macroscopic scale, these affect the mechanical parameters like tensile strength, Young's modulus, and percentage of elongation.

4. FT-IR spectra analysis

Fig. 3 shows Fourier transform infrared spectra of pure PVA film, and PVA–ZnO polymer composite samples where the interactions between dopant and the host PVA polymer matrix are clearly seen. Figure. For the spectra of the PVA film, a strong and broad absorption band at 3334 cm^{-1} is attributed to the O–H stretching vibration. The bands at 2912 and 2940 cm^{-1} are assigned to the C–H stretching vibration of –CH and $–CH_2$, respectively. The peak at 1422 cm^{-1} is designated as a CH_2 scissoring mode, while the peaks at 1374 and 1329 cm^{-1} are attributed to the CH_2 deformation, and the bands at 1093 cm^{-1} and 916 cm^{-1} are due to the C–O and C–C stretching vibrations. The band at 850 cm^{-1} is due to the CH_2 rocking mode.[17]

The moderate absorption peak at 1658 cm^{-1} is assigned to the O–H bending mode of the –OH groups in the PVA.[18] The band at 1235 cm^{-1} is due to the C–O–C vibration in the vinyl acetate group.[19] Notably, the peak at 1143 cm^{-1}, which is related to the C–O stretching vibration in groups at the surface of the ZnO. The stretching vibration of the N–H and the O–H on the surface of the ZnO is located at 3200–3600 cm^{-1}. For the combined action of the N–H, the O–H on the surface of the ZnO and the O–H in the PVA, the peak at 3334 cm^{-1} in the spectra of the PVA/ZnO is far broader than that in the PVA spectra.

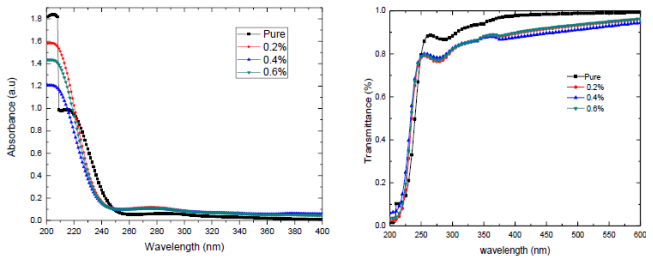

Fig. 4. Absorption and transmittance spectra of (a) pure PVA; (b) PVA–ZnO composite films.

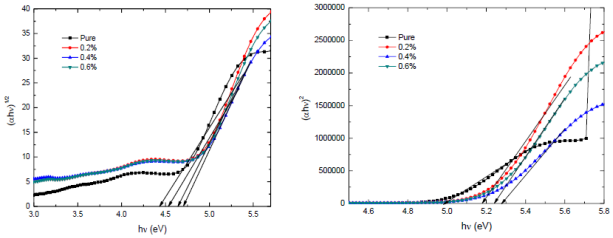

Fig. 5. Direct and Indirect band gap of pure PVA and PVA–ZnO composite films.

5. UV-visible analysis

5.1. Optical properties

The UV–Visible absorption spectroscopy is a widely used technique to examine the optical properties of nano sized particles and hence nanocomposite films. The UV–Visible absorption spectra of pure PVA, nano ZnO and PVA–ZnO nanocomposites over the range 200– 800 nm were recorded using a double beam Cary 5000 UV–Visible spectrometer and are shown in Fig. 4. The absorption spectrum of pure PVA shown in Fig. 4 is characterized by a sharp absorption edge at 241 nm[20] which may indicate either an un-hydrolyzed acetate group in the PVA back bone or the semi crystalline nature of PVA.[21] The optical absorption spectrum of nano ZnO is shown in Fig. 4. The absorption edge in this occurs at 371 nm (3.318 eV) which is blue shifted with respect to characteristic bulk ZnO (380 nm, 3.268 eV) at room temperature.[21] This shift may be due to the quantum confinement effect i.e., due to the reduction in the crystallite size. The absorbance spectrum of PVA–ZnO nanocomposite films is shown in Fig. 4. As indicated in the figure, doping of nano ZnO into PVA matrix has enhanced the absorbance of the PVA host in the UV–Visible region. It is clear that the absorption edge shifts systematically to the higher wavelength or lower energy corresponding to blue–green region of the visible spectral range with increasing concentration of ZnO nanoparticles. The observed red shift in energy may be due to the development of microstrain in PVA–ZnO composite matrix due to the incorporation of dopant ZnO. This strain results in variation in energy band structure of the dopant ZnO and is reflected in the absorption edge shift. Formation of more defect states in the energy gap due to the dopant nano ZnO[22] is also another possible mechanism that may be contributing to the shift.

5.1.1. Determination of optical band gap

The optical transitions in nanocomposite films can be easily understood by determining the optical band gap by translating the

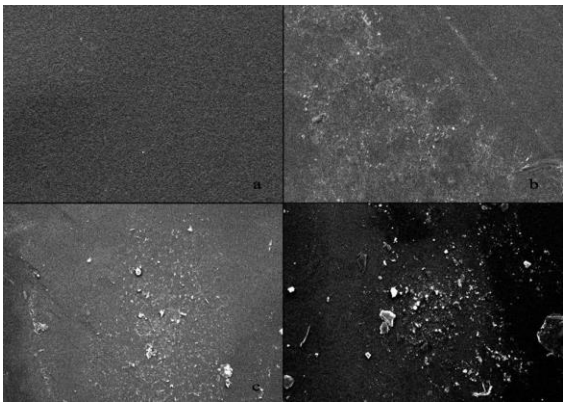

Fig. 6. SEM micrographs of (a) pure PVA (b) PVA–ZnO(0.2%) (c) PVA–ZnO(0.4%) (d) PVA–ZnO(0.6%) composite films.

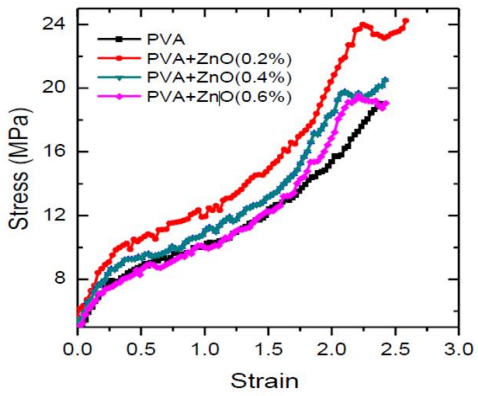

Fig. 7. Stress-strain curves of pure PVA and PVA/ZnO composite films.

UV–Visible spectra into Tauc's plot.[26] The frequency dependent absorption coefficient is given by

$$\alpha(hv) = B(hv - E_g)^r/hv$$

where α is the absorption co-efficient, hv is the incident photon energy, B is the parameter that depends on the inter band transition probability, E_g is the optical band gap and r is an index Characterizing the nature of the electronic transitions causing the optical absorption 'r' can take values 1/2, 3/2, 2, and 3 for direct allowed, direct forbidden, indirect allowed and indirect forbidden transitions, respectively.

Influence of indirect transitions in nanocomposite films due to incorporation of filler PVA-ZnO into polymer matrix is understood by estimating indirect band gap values from the plots of $(\alpha hv)^{1/2}$ versus (hv) as shown in Fig. 6a. Extrapolating the linear portion of the graphs to (hv) axis determines the respective optical energy gap. From Fig. 6a it is clear that the values of indirect band gap increases in energy (from 4.43 eV to 4.70 eV) with increase in doping level. This decrease in band gap may be the result of two mechanisms. The first is the formation of donor levels at the bottom of the conduction band resulting from the tensile strain induced in the composite films. The second is the formation of defects in the polymeric matrix. These defects produce localized states in the optical band gap and these localized states are responsible for increasing energy band gap when dopant (filler) is increased in the polymer matrix.[23] Variation of optical band gap and macrostrain with different dopant concentration are given in Fig. 5. The increase in band gap is directly correlated with increase in strain upto 10 mol%, whereas at 20 mol% the increase in energy gap is larger and both the strain factor as well as the formation of the defect states may be contributing to the observed gap.

6. SEM analysis

The scanning electron micrographs of pure PVA film, ZnO nano powder and ZnO doped PVA films are shown in Fig. 6. SEM of pure PVA at high magnification (Fig. 6a) shows uniformly processed smooth PVA matrix and at low magnification (Fig. 6b) the semi crystalline nature of PVA supporting the observations of XRD analysis.

The micrographs of pure ZnO nano powder (Fig. 6c) show that the particles are made up of agglomeration of many primary crystallites with irregular size and shape which is due to the enormous heat generated during the combustion reaction. Further, the images reveal the presence of voids and pores on the surface of ZnO sample. These pores are attributed to the inherent nature of combustion derived products due to the large amount of gases liberated during the combustion process. The micrograph at higher magnification (Fig. 6d) shows the hexagonal pyramid form associated with quasi platelet structures and the formation of quasi-spherulitic polycrystalline aggregates are also noticed. SEM image of PVA–ZnO composites (Fig. 6) confirm the changes in the morphology of pure PVA with dispersion of ZnO into the polymer matrix. SEM shows uniformly dispersed ZnO, where more compactness exists as concentration of dopant increases indicating more crystalline nature of the sample and the surface is rough compared to pure PVA.[24]

7. Mechanical Test

The mechanical properties were calculated from the plot of stress (tensile force/initial cross-sectional area) versus strain (extension as a fraction of the original length) given in Fig. 7. The mechanical properties were analyzed as a function of ZnO concentrations and tabulated in Table 1.

The tensile strength in the pure PVA film was 14.56 MPa and PVA/ZnO sample, it was 24.44 MPa, 20.58 MPa, 19.75 MPa and in the 0.2 wt%, 0.4 wt%, 0.6 wt%. The extent of reduction in tensile strength varies reduction in the 0.6 wt% concentration; thereby increasing with decreasing the tensile properties. The Elastic modulus (Young's modulus) decreases with increasing as the concentration changes in the 0.6 wt% ZnO concentration, which can be attributed to the reduction of crystallinity. We observe that the percentage of elongation at break decreases with increasing ZnO concentration. Also, we observe that the maximum load (N) decreases with increasing concentration.[25] For food packaging application, the biocomposite films must have good mechanical properties. But from Table 1, we can observe statistically significant decrease with increasing in the mechanical properties of PVA after the incorporation of ZnO composite.

Table 1. Mechanical parameters of pure PVA and PVA/ZnO composite thin films.

Sample	Tensile strength (MPa)	Young's modulus (MPa)	Elongation (%)	Maximum load capacity (N)
Pure PVA	14.56	22.94	96.50	143.71
PVA+0.2wt%ZnO	20.44	27.16	27.16	108.01
PVA+0.4wt%ZnO	24.58	126.79	106.79	096.93
PVA+0.6wt%ZnO	19.75	41.78	41.78	070.04

Table 2. Surface roughness parameters of pure PVA and PVA/ZnO composite films.

Sample	Line Roughness		Area Roughness	
	Ra (nm)	Rq (nm)	Sa (nm)	Sq (nm)
Pure PVA	3.599±0.350	4.743±0.551	3.353±0.172	4.383±0.331
PVA+0.2%ZnO	4.055±0.052	4.860±0.106	3.857±0.655	4.647±0.608
PVA+0.4%ZnO	5.053±0.0837	5.971±0.153	5.055±0.057	5.800±0.137
PVA+0.6%ZnO	8.461±0.370	11.068±0.742	7.863±0.429	9.813±0.771

Where, Ra, Rq – is the Roughness average; Sa, Sq – is the Root means Square (RMS of height distribution)

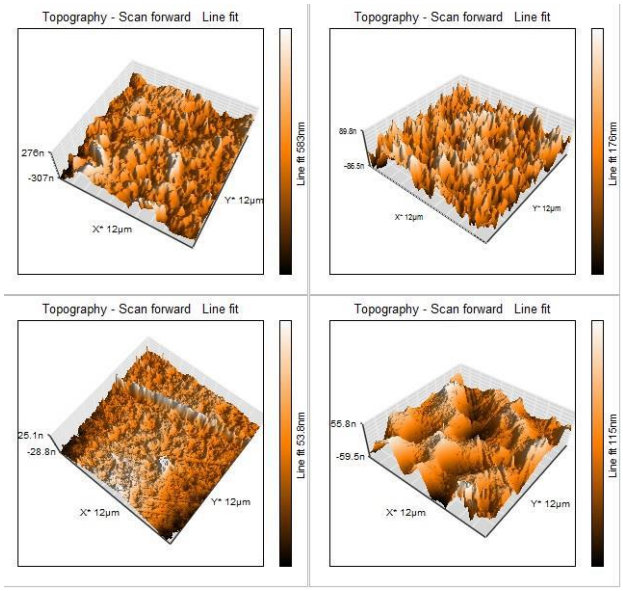

Fig. 8. AFM scans of pure PVA and PVA/ZnO composite films.

8. Surface roughness analysis

Fig. 8 shows the topology and 3D AFM images of virgin and ZnO NPs incorporated polymer samples. The surface topology parameters given in Table 2, present some important physical scales, which morphologically characterize the sample. The line roughness parameters (Ra and Rq) and surface roughness parameters (Sa and Sq) are the physical scales which describe the roughness degree of the samples. From Table 2, it can be seen that, the Surface morphology of different concentration of PVA- ZnO doped composite films analyzed by atomic force microscopy (AFM) is as shown in Fig. These images indicate aggregation/cluster formation of the ZnO at the surface of 0.6 wt. % loaded composite matrix as compared to 0.2 wt. %, which leads to disruption of the charge conduction pathways. This agglomeration could be responsible for the anomalous behavior in conduction mechanism. Since we can see significant change in the surface roughness at the different concentration of PVA-ZnO composite.[26]

9. Conclusions

The basic optical properties and optical constants of the PVA/ZnO composite films have been investigated by means of absorbance and transmittance spectra. The optical constants such as the optical band gap (E_g), of PVA/ZnO composite films were determined. PVA/ZnO composite films have been investigated as a potential technique of refractive index modulating optical elements. The PVA-ZnO Bio-composite films improve the mechanical properties compared to the pure PVA film. Hence, PVA/ZnO Bio-composite films are a promising candidate for packaging materials in the food. The solution casted PVA/ZnO composites containing various wt% of ZnO were prepared and characterized by FTIR and XRD techniques. FTIR peak at 558 cm^{-1} showed the presence of ZnO in the composites. The infrared spectrometry confirmed the presence of ZnO in PVA matrix. XRD showed the crystal structure of ZnO did not altered after preparation of the composites. The surface morphology and morphology of the PVA/ZnO composites films elucidated by AFM and SEM observed that PVA film surface is smoother than other composite films.

Conflicts of Interest

The authors declare no conflict of interest.

References

1 Franklin N.M.; Rogers N.J.; Apte S.C.; Batley G.E.; Gadd G.E.; Casey P.S. Comparative Toxicity of Nanoparticulate ZnO, Bulk ZnO, and $ZnCl_2$ to a Freshwater Microalga (*Pseudokirchneriella subcapitata*): The Importance of Particle Solubility. *Environ. Sci. Technol.*, 2007, **41**, 8484-8490. [CrossRef]

2 Srivastava V.; Gusain D.; Sharma Y.C. Synthesis, Characterization and Application of Zinc Oxide Nanoparticles (n-ZnO). *Ceram. Int.*, 2013, **39**, 9803-9808. [CrossRef]

3 Topoglidis E.; Cass A.E.; O'Regan B.; Durrant J.R. Immobilisation and Bioelectrochemistry of Proteins on Nanoporous TiO_2 and ZnO Films. *J. Electroanal. Chem.*, 2001, **517**, 20-27. [CrossRef]

4 Cooray N.F.; Kushiya K.; Fujimaki A.; Okumura D.; Sato M.; Ooshita M.; Yamase O. Optimization of Al-doped ZnO Window Layers for Large-Area Cu (InGa) Se_2-based Modules by RF/DC/DC Multiple Magnetron Sputtering. *Jpn. J. Appl. Phys.*, 1999, **38**, 6213. [Link]

5 Paneva R.; Gotchev D. Non-linear Vibration Behavior of Thin Multilayer Diaphragms. *Sens. and Actuators A: Phys.*, 1999, **72**, 79-87. [CrossRef]

6 Gao L.; Li Q.; Luan W.; Kawaoka H.; Sekino T.; Niihara K. Preparation and Electric Properties of Dense Nanocrystalline Zinc Oxide Ceramics. *J. Am. Ceram. Soc.*, 2002, **85**, 1016-1018. [CrossRef]

7 Gao P.X.; Ding Y.; Mai W.; Hughes W.L.; Lao C.; Wang Z.L. Conversion of Zinc Oxide Nanobelts into Superlattice-Structured Nanohelices. *Science*, 2005, **309**, 1700-1704. [CrossRef]

8 Rodriguez J.A.; Jirsak T.; Dvorak J.; Sambasivan S.; Fischer D. Reaction of NO_2 with Zn and ZnO: Photoemission, XANES, and Density

Functional Studies on the Formation of NO_3. *J. Phys. Chem. B*, 2000, **104**, 319-328. [CrossRef]
9 Lin H.M.; Tzeng S.J.; Hsiau P.J.; Tsai W.L. Electrode Effects on Gas Sensing Properties of Nanocrystalline Zinc Oxide. *Nanostruct. Mater.*, 1998, **10**, 465-477. [CrossRef]
10 Zhao X.; Zhang S.C.; Li C.; Zheng B.; Gu H. Application of Zinc Oxide Nanopowder for Two-Dimensional Micro-Gas Sensor Array. *J. Mater. Synth. Process.*, 1997, **5**, 227.
11 Hingorani S.; Pillai V.; Kumar P.; Multani M.S.; Shah D.O. Microemulsion Mediated Synthesis of Zinc-Oxide Nanoparticles for Varistor Studies. *Mater. Res. Bull.*, 1993, **28**, 1303-1310. [CrossRef]
12 Trandafilović L.V.; Božanić D.K.; Dimitrijević-Branković S.; Luyt A.S.; Djoković V. Fabrication and Antibacterial Properties of ZnO–Alginate Nanocomposites. *Carbohydr. Polym.*, 2012, **88**, 263-269. [CrossRef]
13 Dong L.F.; Cui Z.L.; Zhang Z.K. Gas Sensing Properties of Nano-ZnO Prepared by Arc Plasma Method. *Nanostruct. Mater.*, 1997, **8**, 815-823. [CrossRef]
14 Ginley D.S.; Bright C. Transparent Conducting Oxides. *MRS Bull.*, 2000, **25**, 15-18. [CrossRef]
15 Hara K.; Horiguchi T.; Kinoshita T.; Sayama K.; Sugihara H.; Arakawa H. Highly Efficient Photon-to-Electron Conversion with Mercurochrome-Sensitized Nanoporous Oxide Semiconductor Solar Cells. *Sol. Energy Mater. Sol. Cells*, 2000, **64**, 115-134. [CrossRef]
16 Keis K.; Vayssieres L.; Lindquist S.E.; Hagfeldt A. Nanostructured ZnO Electrodes for Photovoltaic Applications. *Nanostruct. Mater.*, 1999, **12**, 487-490. [CrossRef]
17 Corso C.D.; Dickherber A.; Hunt W.D. Lateral Field Excitation of Thickness Shear Mode Waves in a Thin Film ZnO Solidly Mounted Resonator. *J. Appl. Phys.*, 2007, **101**, 054514. [CrossRef]
18 Parveen A.; Koppalkar A.K.; Revanasidappa M.; Prasad M.A. Synthesis, Characterization and Electrical Properties of Polyaniline/$SrTiO_3$ Composites, 2009. [Link]
19 Smith P.; Lemstra P.J. Ultrahigh-strength Polyethylene Filaments by Solution Spinning/Drawing, 2. Influence of Solvent on the Drawability. *Die Makromol. Chem.: Macromol. Chem. Phys.*, 1979, **180**, 2983-2986. [CrossRef]
20 Agrawal R.C.; Chandra A.; Bhatt A.; Mahipal Y.K. Investigations on Ion Transport Properties of and Battery Discharge Characteristic Studies on Hot-Pressed Ag+-Ion-Conducting Nano-Composite Polymer Electrolytes:(1–x)[90PEO: $10AgNO_3$]: $xSiO_2$. *New J. Phys.*, 2008, **10**, 043023. [Link]
21 Fernandes D.M.; Silva R.; Hechenleitner A.W.; Radovanovic E.; Melo M.C.; Pineda E.G. Synthesis and Characterization of ZnO, CuO and a Mixed Zn and Cu Oxide. *Mater. Chem. Phys.*, 2009, **115**, 110-115. [CrossRef]
22 Dai L.; Li J.; Yamada E. Effect of Glycerin on Structure Transition of PVA/SF Blends. *J. Appl. Polym. Sci.*, 2002, **86**, 2342-2347. [CrossRef]
23 Seoudi R.; El-Bailly A.B.; Eisa W.; Shabaka A.A.; Soliman S.I.; Abd El Hamid R.K.; Ramadan R.A. Synthesis, Optical and Dielectric Properties of (PVA/ CdS) Nanocomposites. *J. Appl. Sci. Res.,* 2012, **8**, 658-667. [Link]
24 Dutta S.; Ganguly B.N. Characterization of ZnO Nanoparticles Grown in Presence of Folic Acid Template. *J. Nanobiotechnol.*, 2012, **10**, 1-10. [CrossRef]
25 Hemalatha K.S.; Rukmani K.; Suriyamurthy N.; Nagabhushana B.M. Synthesis, Characterization and Optical Properties of Hybrid PVA–ZnO Nanocomposite: A Composition Dependent Study. *Mater. Res. Bull.*, 2014, **51**, 438-446. [CrossRef]
26 Roy A.S.; Gupta S.; Sindhu S.; Parveen A.; Ramamurthy P.C. Dielectric Properties of Novel PVA/ZnO Hybrid Nanocomposite Films. *Compos. Part B: Eng.*, 2013, **47**, 314-319. [CrossRef]